Ionization of laser-excited strontium vapor: The dynamics of superelastic collisions with metastable populations

C. Bréchignac, Ph. Cahuzac, and A. Débarre
Laboratoire Aimé Cotton, CNRS II, Bâtiment 505, F-91405 Orsay Cédex, France*
(Received 25 June 1984)

We report on the observation and absolute measurements of the population dynamics for several Sr I and Sr II levels when the vapor is illuminated by a short laser pulse. When the laser beam excites the $5s\,5p\ ^1P_1$ resonance level, we show that a pool of metastable population is created, allowing an efficient heating of the medium by superelastic collisions with seed electrons, and a strong final ionization is achieved. When the laser source excites the $5s\,10s\ ^1S_0$ Rydberg level, superelastic collisions do not occur and a drastic change in the population behavior is observed. In both cases the dynamics of the energy transfer towards the plasma is detailed.

I. INTRODUCTION

The ionization of a dense metal vapor illuminated by a resonant laser frequency has been first investigated by Lucatorto and McIlrath.[1] The observed ionization rate reaches 95% of the initial excited-level population. Assuming that the ionization process is dominated by superelastic collisions, Measures and Cardinal proposed a model[2] which is able to predict the evolution of the ionization rate of the medium when a steady population is stored on the resonance level. They predicted that, in this case, a delay is necessary to reach the burnout stage leading to runaway ionization of the medium. Further theoretical and experimental investigations[3–11] have clearly confirmed the major role played by superelastic collisions in which seed electrons gain energy by collisions with excited atoms. These electrons are in turn able to excite and to ionize the atoms of the vapor. Thus the redistribution of the initial energy in the system depends mostly on the mechanisms of heating and cooling of the electrons.

Up to now the time evolution of such a system has only been investigated during a long laser pulse when the resonance level is continuously fed and the observed ionization results from both collisional and optical processes. The various experiments have used either ion[6–8] or electron[9] detections or optical diagnostics of the plasma.[1,3–5,7,10] The first method allows us to detect ions or electrons that have drifted out of the plasma region, whereas the last one allows us to study *in situ* the dynamics of the ionization.

We report here the results of time evolution of strontium-level populations after a short resonant laser-pulse excitation. The aim of our experiment is to follow in time the excitation and ionization energy transfer by superelastic collisions, free of multiphoton processes, and not to obtain a very high ionization rate of the vapor. Preliminary results have already been reported using either a direct excitation of the resonance level or two-photon excitation to the Rydberg level $5s\,10s\ ^1S_0$.[10] A delay to reach the maximum ionization is clearly put into evidence and the role of seed electrons is discussed. In the present work, the dynamics study is performed by delayed-absorption measurements. The method applied to the main relevant levels of the system is described in the Sec. II.

By this way we have determined the population time history of six low-lying levels of neutral strontium including the metastable levels. We have extended the measurements to the ground and resonance levels of Sr^+. The results, which are reported in Sec. III, are completed by time-resolved fluorescence observations especially from high-lying strontium levels. We clearly put into evidence the role played by various excited levels of neutral Sr in the ionization process and especially the energy-storage character of metastable ones. A qualitative interpretation is given in Sec. IV.

All the active atoms may be involved in superelastic collisions which heat and ionize the medium. They must play a large role and even predominate in cell experiments where intense illumination of a resonance transition is achieved as soon as the density of excited atoms provides a large energy reservoir.

II. EXPERIMENTAL METHOD

The scheme of the experimental setup is shown in Fig. 1. Two co-propagating laser beams are superimposed in a cell which contains 1 Torr pressure of strontium vapor and 30 Torr of krypton as buffer gas. These two beams are provided by two dye lasers simultaneously pumped by a N_2 laser and the pulse duration is 7 ns. The pump beam of a few MW/cm^2 peak power is tuned either to the resonance line at 460.7 nm [Fig. 2(a)] or to the two-photon transition $5s^2\ ^1S_0 \rightarrow 5s\,10s\ ^1S_0$ at 459.5 nm [Fig. 2(b)] and surrounds the weak beam that probes the central part of the excited medium. The cross-sectional area of the laser-pumped volume is 10^{-3} cm^{-2}. The probe beam can be delayed by passing through an optical delay line using a mirror arrangement initially described by White.[12] This 40-cm-long delay line allows us to vary step by step (5.3 ns) the delay from 8 to 270 ns. The absorbed probe beam is sent into a photomultiplier and analyzed through a syn-

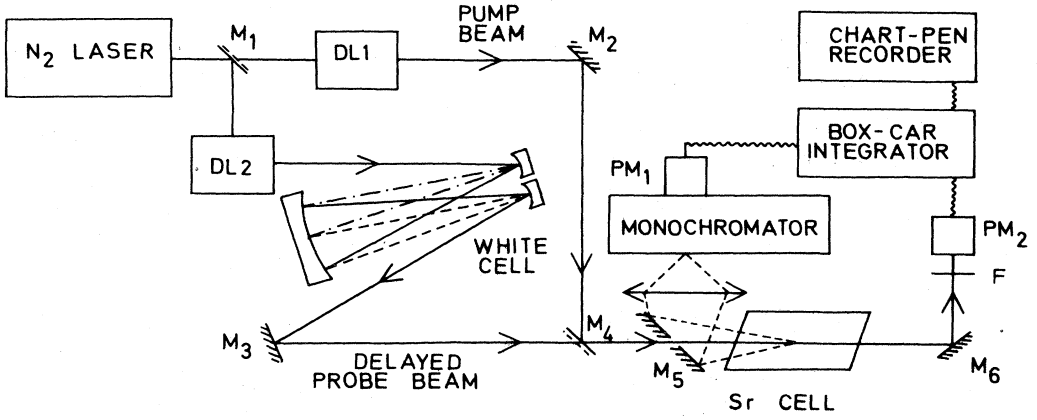

FIG. 1. Schematic of the experimental setup. $DL1$, $DL2$, dye lasers; M_1, M_4, dichroic mirrors; M_5, pierced mirror; F, filter to suppress the pump laser light; PM_1, PM_2, photomultipliers for fluorescence or absorption studies, respectively.

chroneous gated detector.

Six levels have been probed by the delayed-absorption method in neutral strontium: the ^3P and ^3D metastable ones (unless the $^3P_0$ and $^3D_1$ levels), the $5s4d\ ^1D_2$ level, and the resonance one (Fig. 2). For Sr^+ the relevant levels are the ground and resonance ones. The metastable levels of Sr^+ which require either infrared or uv wavelengths have not been probed.

To complete the description of the system, emission measurements have also been performed from highly excited levels. The corresponding transitions are tabulated in Table I.

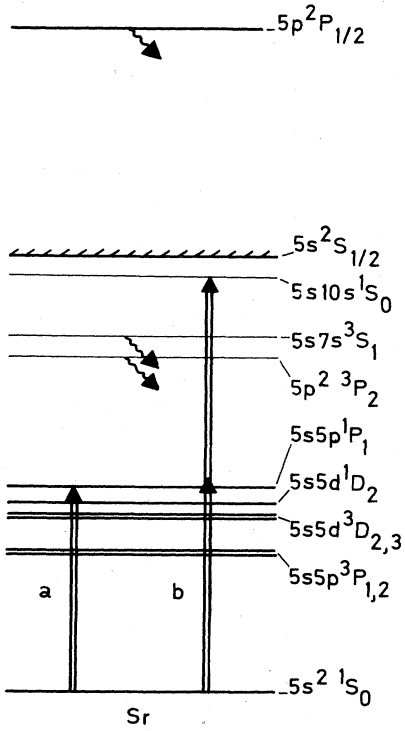

FIG. 2. Energy diagram of the relevant levels in Sr and Sr^+. The levels drawn with heavy lines have been probed by the delayed-absorption method. Levels marked by wavy arrows deal with time-resolved fluorescence analysis. (a) Pump laser at 460.7 nm; (b) pump laser at 459.5 nm.

A. Absorption measurements

Under experimental conditions well determined by the metallic vapor density, the frequency of the pump laser, and the optical delay, an absorption profile for a given transition is obtained by recording the transmitted intensity of the probe beam when it is tuned across this transition. The population dynamics of its lower level is deduced by recording absorption profiles for various optical delays. Following our previous experiment we choose our experimental conditions—partial pressures of Sr and buffer gas Kr—to have a characteristic diffusion time for Sr atoms out of the plasma region of a few tens of μs, much larger than the delay time for maximum ionization [240 ns, as it is shown by the time evolution of the resonance ion fluorescence, Fig. 5(a)].[10] The global neutrality of the ionized medium ensures a long lifetime to the plasma in which strontium ions are confined by electrostatic interaction with electrons. This stability is confirmed by the observation of large delays for the maximum of the resonance ion fluorescence, which can reach 14 μsec at low strontium vapor pressure.

As it is well known, when the population density N_1 of the lower level of a transition is much larger than the upper one, N_2, N_1 is simply related to the absorption coefficient

$$\int k(\nu)d\nu = \frac{\lambda^2}{8\pi}\frac{g_2}{g_1}A_{21}N_1 , \tag{1}$$

where λ is the wavelength of the transition, g_1 and g_2 the statistical weights of the levels, and A_{21} the Einstein coefficient for spontaneous emission. The $k(\nu)$ coefficient is easily deduced from the measurement of the relative absorption of the probe beam

TABLE I. List of the transitions involved in our measurements. *a* and *b* correspond, respectively, to the pump-laser wavelength at 460.7 and 459.5 nm as indicated in Fig. 2. Symbols in the last column stand for delayed-absorption measurements (*A*) and time-resolved fluorescence measurements from the upper level in the absence of the probe beam (*E*).

Wavelength (Å)	Transition		Observation	Pump laser
4077.7	$5s\,^2S_{1/2}-5p\,^2P_{3/2}$	Sr II	*E*	*a,b*
4158.5	$5s4d\,^1D_2-5s8f\,^1F_3$	Sr I	*A*	*a*
4161.7	$5s4d\,^1D_2-5s\,8f\,^3F_{1,2,3}$	Sr I	*A*	*a*
4161.8	$5p\,^2P_{1/2}-6s\,^2S_{1/2}$	Sr II	*A*	*a*
4215.5	$5s\,^2S_{1/2}-5p\,^2P_{1/2}$	Sr II	*A,E*	*a,b*
4438.0	$5s5p\,^3P_2-5s\,7s\,^3S_1$	Sr I	*E*	*a,b*
4722.3	$5s5p\,^3P_1-5p^2\,^3P_2$	Sr I	*E*	*a*
4784.3	$5s5p\,^3P_1-5p^2\,^3P_1$	Sr I	*E*	*a*
4811.9	$5s5p\,^3P_2-5p^2\,^3P_2$	Sr I	*A,E*	*a,b*
4868.7	$5s4d\,^3D_2-5s4f\,^3F_3$	Sr I	*A*	*a,b*
4869.2	$5s4d\,^3D_2-5s4f\,^3F_2$	SrI	*A*	*a*
4872.5	$5s\,5p\,^3P_1-5s\,5d\,^3D_2$	Sr I	*A,E*	*a,b*
4876.1	$5s\,5p\,^3P_1-5s5d\,^3D_1$	Sr I	*A,E*	*a,b*
4876.3	$5s5p\,^3P_2-5p^2\,^3P_1$	Sr I	*A*	*a,b*
4892.0	$5s4d\,^3D_3-5s4f\,^3F_4$	Sr I	*A*	*a,b*
4892.6	$5s4d\,^3D_3-5s4f\,^3F_3$	Sr I	*A*	*a*
5229.3	$5s4d\,^3D_2-4d5p\,^3P_2$	Sr I	*E*	*a*
5156.1	$5s4d\,^1D_2-5s4f\,^1F_3$	Sr I	*E*	*a*
5329.8	$5s4d\,^1D_2-5s7p\,^1P_1$	Sr I	*E*	*a*
6546.8	$5s4d\,^3D_3-4d5p\,^3F_3$	Sr I	*A,E*	*a*
6550.3	$5s\,5p\,^1P_1-5p^2\,^1D_2$	Sr I	*A,E*	*a*

$$I(\nu)=I_0\exp[-k(\nu)l]\,, \tag{2}$$

where l is the active length of the probed column, I_0 is the incident probe flux, and $I(\nu)$ the transmitted one as a function of the probe frequency ν. In the particular case of weak absorption $k(\nu)$ and $I(\nu)$ are linearly dependent and a straightforward calculation[13] shows that

$$\int k(\nu)d\nu=\frac{1}{l}\frac{\mathscr{A}}{I_0}\,, \tag{3}$$

where $\mathscr{A}$ is the absorption area

$$\mathscr{A}=\int [I_0-I(\nu)]d\nu\,, \tag{4}$$

a quantity which depends neither on the absorption-line profile nor on the laser-line profile. In the case of a relatively large absorption, the linear approximation is no longer valid. However, Eq. (3) is still useful by considering the effective absorption profile deduced from Eq. (2). Actually, the sensitivity of the method is limited by the intensity fluctuations of the background signal I_0, and relative absorptions larger than 5% are considered.

A difficulty arises for a strong saturated absorption. In such a situation, the above procedure is no longer valid. This case concerns only the resonance line for which the resonant broadening predominates leading to a Lorentzian absorption profile for the far wings. However, it is still possible to deduce an order of magnitude for N_1 from the analysis of the far-wings unsaturated absorption profiles and from the *a priori* calculation of the homogeneous linewidth.

B. Emission measurements

In the case of very low populated levels leading to a very weak absorption, it is convenient to record the time evolution of the fluorescence when the probe beam is switched off. This method is meaningful for optically thin lines involving upper levels for which the lifetime is short enough, so that the time evolution of the fluorescence will reproduce the excitation rate of the level. This is especially the case for highly excited levels of neutral strontium and also for the resonance level of Sr^+. The corresponding transitions are listed in the Table I.

TABLE II. Calculated transition probabilities for several lines of strontium.

Transition	gA (s^{-1})
$5s\,5p\,^1P_1-5p^2\,^1D_2$	6.08×10^8
$5s\,5p\,^1P_1-5s\,10s\,^1S_0$	0.02×10^8
$5s4d\,^1D_2-5s8f\,^1F_3$	0.68×10^8
$5s4d\,^3D_3-5s4f\,^3F_4$	10.84×10^8
$5s4d\,^3D_3-5s4f\,^3F_3$	0.94×10^8
$5s4d\,^3D_3-4d5p\,^3F_3$	0.47×10^8
$5s4d\,^3D_2-5s4f\,^3F_3$	7.61×10^8
$5s4d\,^3D_2-5s4f\,^3F_2$	0.95×10^8
$5s5p\,^3P_2-5p^2\,^3P_2$	11.30×10^8
$5s5p\,^3P_2-5p^2\,^3P_1$	3.62×10^8
$5s5p\,^3P_1-5s5d\,^3D_2$	1.26×10^8
$5s5p\,^3P_1-5s5d\,^3D_1$	0.42×10^8
$5s\,^2S_{1/2}-5p\,^2P_{1/2}$	2.75×10^8

TABLE III. Population densities in 10^{13} atoms/cm^3 units deduced from absorption measurements and transition-probability calculations. *a* and *b* stand for pump-laser wavelength at 460.7 and 459.5 nm, respectively.

		τ(ns)	0	8	13	30	56		110		163	216	243	270
		Levels												
a	Sr I	$5s5p\ ^1P_1$	25.60	0.62	0.50	0.34	0.23		0.12		0.10	0.09		
		$5s4d\ ^1D_2$		9.80	9.21		1.53							
		$5s4d\ ^3D_3$		1.01		1.13	1.16		1.09			0.77	0.61	
		$5s4d\ ^3D_2$		1.36		0.58	0.63		0.52				0.32	
		$5s5p\ ^3P_2$		0.18		0.27	0.30		0.28				0.12	
		$5s5p\ ^3P_1$		0.64		1.49	1.84		1.83				0.82	
	Sr II	$5s\ ^2S_{1/2}$	0.01	0.01		0.05	0.15	0.30	0.25	0.34	0.41	0.48		0.54
		$5p\ ^2P_{1/2}$											$n(\max) < 0.01$	
b	Sr I	$5s4d\ ^3D_3$				<0.02						0.05		
		$5s4d\ ^3D_2$				<0.03						0.08		
		$5s5p\ ^3P_2$				<0.02						0.05		
		$5s5p\ ^3P_1$				<0.03						0.05		
	Sr II	$5s\ ^2S_{1/2}$			0.02	0.10	0.12	0.11	0.05	0.10		0.09		0.08

An absolute calibration of these measurements is possible in terms of population densities if, for a given level, absorption and fluorescence analysis are available. This is done for the $5p\ ^2P_{1/2}$ ion level (see Sec. IV).

III. EXPERIMENTAL RESULTS

A. Transition-probability calculations

The values of N_1 deduced from the absorption-line analysis rely on the transition probabilities A_{21}. There are no values available in the literature for most of the relevant transitions. The values listed in Table II have been calculated by a central field method using the parametric potential developed by Klapisch.[14] These levels have been described in a pure *L-S* coupling scheme. We have not taken into account the configuration interactions which mainly affect the singlet levels. Consequently, a better accuracy is expected for the transitions involving triplet levels. A large uncertainty affects the probabilities for the transitions involving the $5s5p\ ^1P_1$ and $5s4d\ ^1D_2$ since a pure *L-S* coupling is not very well suited to describe these levels.

B. Time evolution of the population densities

The experimental values of the population density deduced from the delayed-absorption measurements and the calculated transition probabilities are listed in Table III. The experimental uncertainty on N_1 is of the order of 25%, but the absolute values also depend on the accuracy of A_{21}. A rough estimate of the absolute ground-state population when the pump laser is switched off leads to a density of 10^{15} atoms/cm^3, whereas the value deduced from temperature leads to a few 10^{15} atoms/cm^3.

The behavior of the system as a whole is depicted in Figs. 3 and 4. In Fig. 3 is displayed the time evolution of the level populations involved in the ionization process

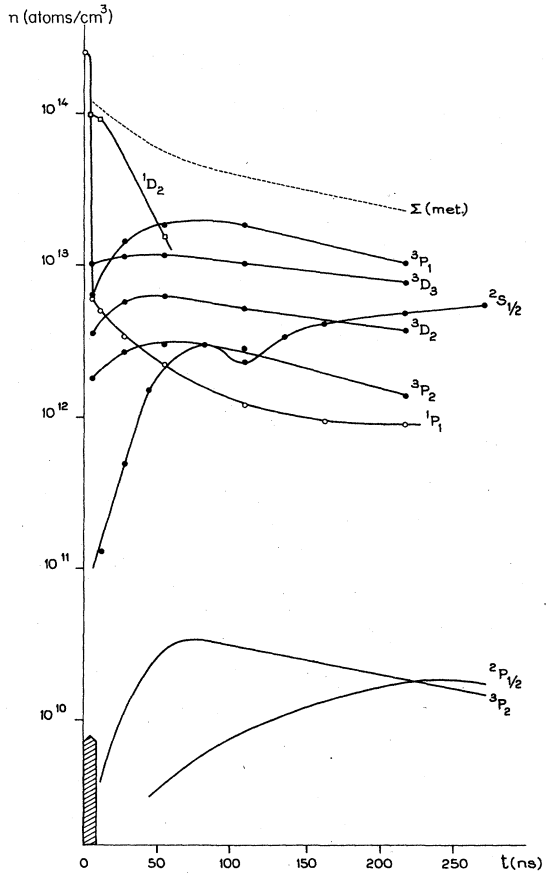

FIG. 3. Time evolution of the Sr and Sr^+ levels when the pump-laser wavelength is $\lambda = 460.7$ nm. The dots correspond to delayed-absorption measurements from the $5s5p\ ^1P_1, ^3P_{1,2}$ and $5s4d\ ^1D_2, ^3D_{2,3}$ levels. The dashed line corresponds to the sum of the metastable populations, including the $^{1,3}D$ ones. The solid lines without dots are deduced from time-resolved fluorescence analysis of the $5p^2\ ^3P_2$ level of Sr and for the resonance population of Sr^+. Dashed arrow: laser-pulse duration.

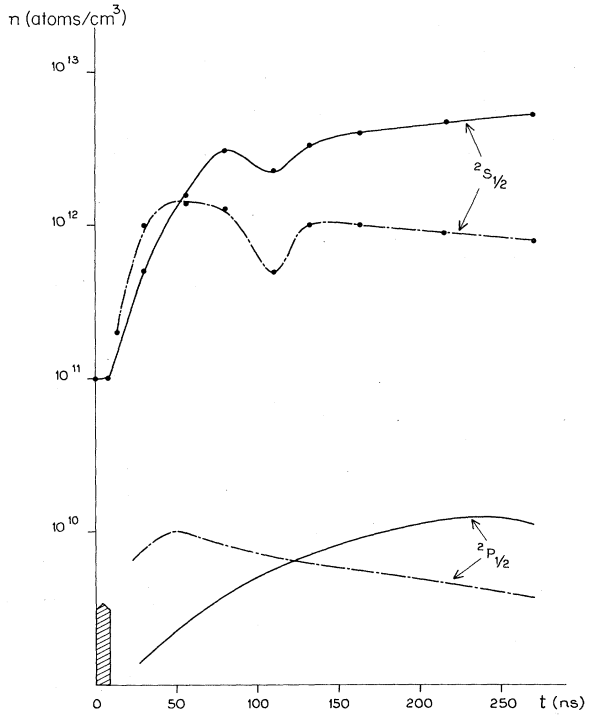

FIG. 4. Comparative evolutions of the ground and resonance populations of Sr^+ when the pump laser is tuned either to 460.7 nm (solid lines) or to 459.5 nm (dot-dashed lines). Dashed arrow: laser-pulse duration.

when the pump laser is tuned to the $5s5p\ ^1P_1$ resonance level. Figure 4 is devoted to a comparative evolution of the Sr^+-level populations when the laser is tuned either to 460.7 nm or to 459.5 nm. The difference in the time behavior of ionization depends whether or not a finite pool of energy is stored on the $5s5p\ ^3P$ and $5s4d\ ^3D$ Sr levels. Although roughly the same rate of ionization is achieved in both cases, the mechanisms are quite different. When the laser is tuned to the Rydberg $5s10s\ ^1S_0$ level, associative (or pooling) ionization could be evoked[10] to understand such an ionization and a relatively short delay is observed. On the contrary, when the laser is tuned to the resonance $5s5p\ ^1P_1$ level, a longer delay time is observed to obtain the maximum rate of ionization. In this later case, the main result is that with an initial metastable atomic density of 10^{14} atoms/cm^3 and a seed electron density of about 10^{11} cm^{-3}, one reaches an ion density of the order of 10^{13} ions/cm^3.

IV. INTERPRETATION OF THE RESULTS

A. Pump laser at 460.7 nm

During the short laser excitation, the resonance $5s5p\ ^1P_1$ level is strongly populated, while a pool of seed electrons is created. Multiphoton ionization could be the major source responsible for this fast ionization, although various processes have been invoked.[8] The initial electron density does not exceed 10^{11} cm^{-3} (see Fig. 3). The fast decay observed for the resonance population is probably due to a superradiant emission at $\lambda=6.45$ μm which strongly populates the $5s4d\ ^1D_2$ level. Although we did not observe directly this emission, the $5s5p\ ^1P_1$–$5s4d\ ^1D_2$ transition is a good candidate for such a process, since it has been already observed as a strong laser line.[15,16] When the laser is switched off, the energy is transferred to the $5s5p\ ^3P$ metastable levels by radiative decay and to the $5s4d\ ^3D$ levels by collisional deexcitation. After a delay of the order of 60 ns, a large fraction of the initial population is stored in the manifold of "metastable" levels, including the $^{1,3}D$ ones. The other part of the resonance population is lost via the trapped fluorescence at 460.7 nm. The whole metastable population is an energy reservoir which is slowly decreasing in time.

This loss of metastable population results from superelastic collisions which then can take place:

$$\mathrm{Sr(metastable)}+e^-(\epsilon)\rightarrow \mathrm{Sr}(5s^2\ ^1S_0)+e^-(\epsilon'>\epsilon)\ . \quad (5)$$

The electron energy ϵ is increased. In turn hot electrons are able to excite the manifold of high-lying $\mathrm{Sr}(n,l)$ levels:

$$\mathrm{Sr(metastable)}+e^-(\epsilon')\rightarrow \mathrm{Sr}(n,l)+e^-(\epsilon''<\epsilon')\ . \quad (6)$$

As a consequence of the heating of the medium by superelastic collisions, the energy climbs throughout the highly excited levels until the ground level of the ionized strontium is reached. Actually, seed electrons may undergo several successive superelastic collisions and their energy becomes sufficient to provide a direct collisional ionization from the resonance state, avoiding the intermediate levels. We note also that these intermediate states behave in time like the metastable ones. Their transient population results from a balance between the electronic excitation from the strongly populated metastable states, a fast radiative decay, and a small leakage to the continuum. Then the active atoms loop between the two manifolds.

At this stage of the process, because the recombination phenomena have a very long time constant as compared to the other ones, the energy is stored on the ground state of the ionized strontium. This is reflected by the slowly increasing population of this level during the observed time range. Obviously, hot electrons are still present and electronic collisions lead to the excitation of the resonance level of Sr^+:

$$\mathrm{Sr}^+(5s\ ^2S_{1/2})+e^-(\epsilon'')\rightarrow \mathrm{Sr}^+(5p\ ^2P)+e^-(\epsilon'''<\epsilon'')\ . \quad (6')$$

In other words, the ground level of Sr^+ constitutes also an energy reservoir, a role quite similar to the one of the metastable Sr population. Because the energy reservoir is not infinite, for a longer delay, heating processes are balanced by cooling ones and this corresponds to the maximum observed for the $5p\ ^2P$ resonance population at 240 ns.

B. Pump laser at 459.5 nm

When the pump laser is tuned on resonance with the $5s10s\ ^1S_0$ level other remarkable features occur: absorption measurements show that the population densities of all the observed levels of the neutral strontium are very weak, in the 0–200-ns time range. This is not surprising since the resonance level is not directly excited and the

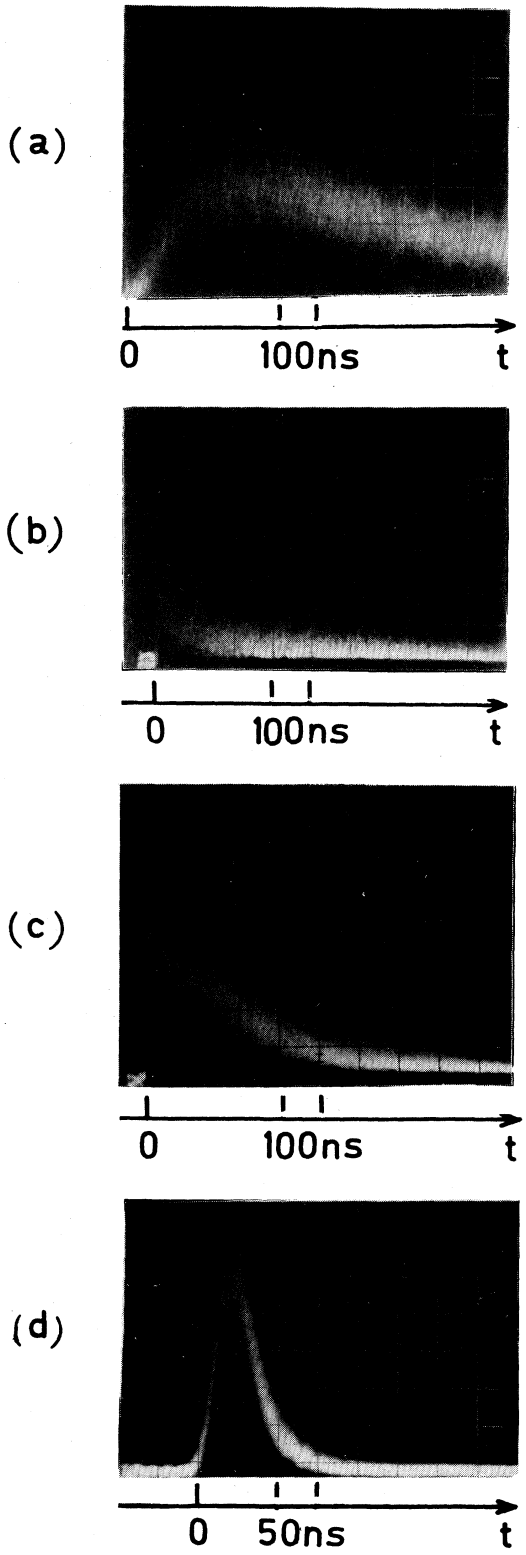

FIG. 5. Time evolution of the fluorescence line ($\lambda=407.8$ nm): (a) pump laser at 460.7 nm, (b) pump laser at 459.5 nm. Time evolution of the $5s7s\ ^3S_1$ fluorescence ($\lambda=443.8$ nm): (c) pump laser at 460.7 nm, (d) pump laser at 459.5 nm. Intensities not to scale.

rather limited population of the $5s10s\ ^1S_0$ level is distributed over a large number of states. At the early stage of the process, the ionization rate is of the same order of magnitude as in the case of the excitation at $\lambda=460.7$ nm. However, the ionization density takes a maximum at $t\simeq 60$ ns and slowly decreases. In addition a deep hole is observed at $t\simeq 110$ ns. This feature which is also present, but less pronounced in the other excitation scheme, is not yet understood.

These observations may be explained as the following. Since there is no energy reservoir, the conditions are not suitable for superelastic collision processes and the seed electrons created either during the laser pulse by multiphoton ionization or by energy pooling cannot gain energy. The initial ionization density slowly vanishes because of recombination processes. On the contrary, when superelastic collisions are present, heating processes overcompensate this loss of ionization and the population of the $5s\ ^2S_{1/2}$ level increases with the delay. This quasisymmetrical behavior is well depicted in Fig. 4. This interpretation is also in agreement with the short delay observed for the maximum of the $5p\ ^2P_{1/2}$ fluorescence intensity.

The fluorescence study of Fig. 5 completes, for a more extended range (0—900 ns), the results of Figs. 3 and 4. Especially, we note the different behaviors of the fluorescence at $\lambda=443.8$ nm depending on the pump-laser wavelength. When the laser excites the $5s10s\ ^1S_0$ level, no spikes are observed in the fluorescence which is short in time and free of any long tail. This indicates that in such a situation the population of this level is not due to superelastic collisions[10] but results from radiative decays or from atom-atom collisional energy transfer.

V. CONCLUSION

By using a double optical resonance method we have disentangled the mechanism allowing the energy transfer from the metastable manifold to the resonance ion level via the ground ion state. The role of the metastable levels is clearly established, a role already invoked in ionization of barium and strontium vapors and which drastically distinguish alkaline-earths vapors from alkaline ones. In the light of our experimental results, two independent steps in the process can be distinguished: (i) the energy transfer from the metastable levels of neutral strontium into the ion storage level, (ii) the electronic excitation into the resonant ion level from the ground one.

We also demonstrated that despite the short pulsed excitation the medium is efficiently ionized: 2 orders of magnitude are gained as compared to the direct multiphoton ionization at $\lambda=460.7$ nm and even more the efficiency is larger than in the case of ionization at $\lambda=459.5$ nm, although in the $5s10s\ ^1S_0$ excitation case the efficient associative ionization is predominant. However, the use of short laser pulses is quite suitable for the study of collisional mechanisms, but the limited value of the energy deposited in the medium hinders a complete burn out, contrary to the case of long laser pulses.

Two among the whole described phenomena are not yet understood: the anomalous long delay observed for the

ionization process with the direct excitation of the $5s10s\ ^1S_0$ level and the dip which exists in the time evolution of the ground ionic population. This later phenomenon could result from the electronic excitation of the metastable levels in the ionized strontium.

Propagation effects or refractive index effects of the laser pulse in such a dense medium have not been taken into account. They should give rise to inhomogeneity effects in the beam-shaped volume when the strong resonance line is excited. This consideration and even more the important role devoted to the storage of energy in the metastable levels suggest the consideration of the intercombination line $5s^2(^1S_0)\rightarrow 5s5p(^3P_1)$ at $\lambda=689.2$ nm as another good candidate for such studies. This is a direct way to excite selectively the lowest metastable levels $5s5p\ ^3P_J$ and the transition probability is weak enough to prevent propagation effects or refractive index effects. These investigations are now in progress.

ACKNOWLEDGMENTS

The authors wish to thank Dr. M. Aymar for her help in the transition-probability calculations.

---

*Laboratoire associé à l'université Paris—Sud.

[1]T. B. Lucatorto and T. J. McIlrath, Phys. Rev. Lett. **37**, 428 (1976).
[2]R. M. Measures and P. G. Cardinal, Phys. Rev. A **23**, 801 (1981).
[3]T. J. McIlrath and T. B. Lucatorto, Phys. Rev. Lett. **38**, 1390 (1977).
[4]A. C. Tam and W. Happer, Opt. Commun. **21**, 403 (1977).
[5]C. H. Skinner, J. Phys. B **13**, 55 (1980).
[6]T. Stacewicz, Opt. Commun. **35**, 239 (1980).
[7]H. A. Bachor and M. Kock, J. Phys. B **14**, 2793 (1981).
[8]B. Carré, F. Roussel, P. Breger, and G. Spiess, J. Phys. B **14**, 4289 (1981).
[9]J. L. Le Gouët, J. L. Picqué, F. Wuilleumier, J. M. Bizau, P. Dhez, P. Koch, and D. L. Ederer, Phys. Rev. Lett. **48**, 600 (1982).
[10]C. Bréchignac and Ph. Cahuzac, Opt. Commun. **43**, 270 (1982).
[11]L. Jahreiss and M. C. E. Huber, Phys. Rev. A **28**, 3382 (1983).
[12]J. U. White, J. Opt. Soc. Am. **32**, 285 (1942).
[13]R. Damaschini (private communication).
[14]M. Klapish, Comput. Phys. Commun. **2**, 239 (1971).
[15]Ph. Cahuzac, J. Phys. (Paris) **32**, 499 (1971).
[16]C. Bréchignac and Ph. Cahuzac, J. Phys. B **14**, 221 (1981).

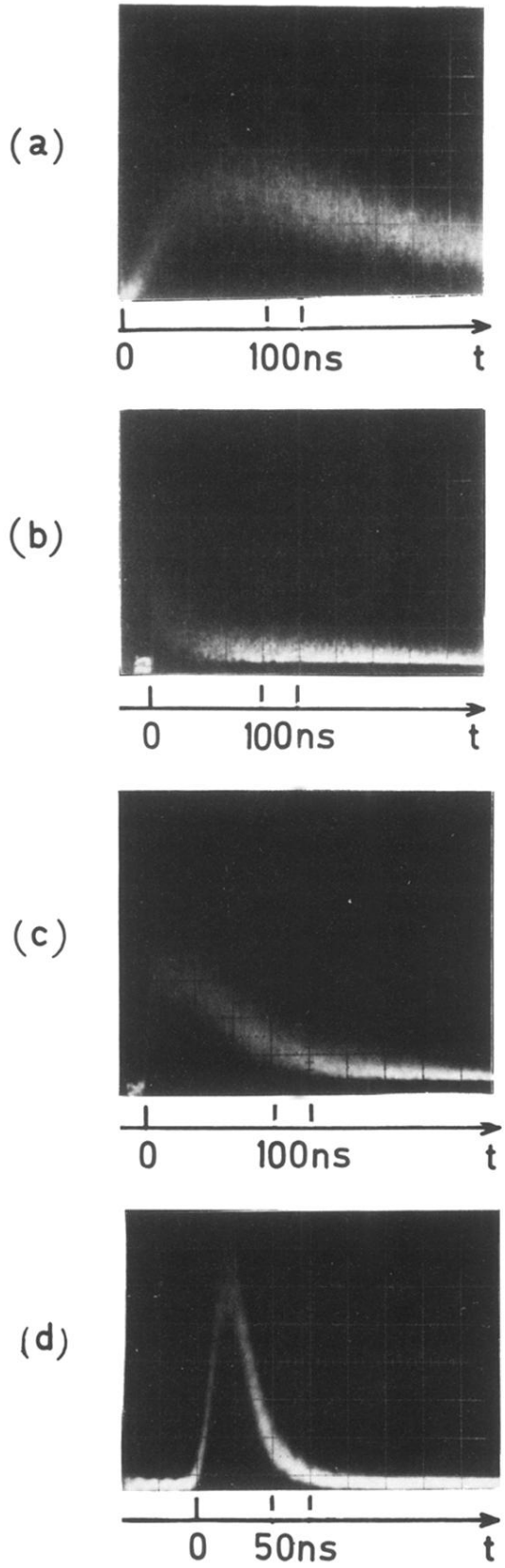

FIG. 5. Time evolution of the fluorescence line ($\lambda = 407.8$ nm): (a) pump laser at 460.7 nm, (b) pump laser at 459.5 nm. Time evolution of the $5s7s\ ^3S_1$ fluorescence ($\lambda = 443.8$ nm): (c) pump laser at 460.7 nm, (d) pump laser at 459.5 nm. Intensities not to scale.